A polymeric two-dimensional mixed-metal network. Crystal structure and magnetic properties of $\{[P(Ph)_4][MnCr(ox)_3]\}_n$

Silvio Decurtins*, Helmut W. Schmalle and Hans Rudolf Oswald
Institut fur Anorganische Chemie, Universität Zurich, Winterthurerstrasse 190, 8057 Zurich (Switzerland)

Anthony Linden
Institut fur Organische Chemie, Universitat Zurich, Winterthurerstrasse 190, 8057 Zurich (Switzerland)

Jürgen Ensling and Philipp Gütlich
Institut fur Anorganische Chemie und Analytische Chemie, Johannes Gutenberg-Universitat Mainz, Staudinger Weg 9, 55099 Mainz (Germany)

Andreas Hauser
Institut fur Anorganische und Physikalische Chemie, Universitat Bern, Freiestrasse 3, 3009 Bern (Switzerland)

(Received August 27, 1993)

Abstract

The mixed-metal ferromagnet $\{[P(Ph)_4][MnCr(ox)_3]\}_n$, where Ph is phenyl and ox is oxalate, has been prepared and a two-dimensional network structure, extended by Mn(II)–ox–Cr(III) bridges, has been determined from single crystal X-ray data. Crystal data: space group *R3c*, $a = b = 18.783(3)$, $c = 57.283(24)$ Å, $\alpha = \beta = 90$, $\gamma = 120°$, $Z = 24$ ($C_{30}H_{20}O_{12}PCrMn$). The magnetic susceptibility data obey the Curie-Weiss law in the temperature range 260–20 K with a positive Weiss constant of 10.5 K. The temperature dependence of the molar magnetization exhibits a magnetic phase transition at $T_c = 5.9$ K. The structure is discussed in relation to the strategy for preparing molecular based ferromagnets and, in addition, it is a solution to the question of the dimensionality of the $[MM'(ox)_3]_n$ network, which in principle can extend two- or three-dimensionally to the crystal lattice. The optical absorption spectra of the single crystals are assigned to the 'CrO_6' chromophores. Their polarization patterns reflect the electric dipole selection rules for D_3 symmetry. A strong site selective luminescence from the chromium(III) ^2E states is observed at low temperature and the system may be suitable for studying energy transfer mechanisms.

Key words. Crystal structures; Magnetism; Manganese complexes; Chromium complexes, Dinuclear complexes

Introduction

The synthesis and study of polymetallic complexes with the goal to design molecular based ferromagnets has been the subject of numerous studies in recent years [1–9]. One strategy along this line consists of synthesizing structurally ordered bimetallic chains or layers with two different paramagnetic ions. Within these extended units either a parallel alignment of the local spins based on symmetry conditions may be realized or, as is most frequently the case, an antiferromagnetic interaction between the adjacent metal ion pairs leads to a ferrimagnetic state because of the non-compensation of the local spins. However the crucial step in the realization of a ferromagnetic compound is the control of interchain or interlayer interactions, which are always very weak so that, at most, a low critical temperature (T_c) for a magnetic phase transition may result. One way to enhance the T_c value could be by the synthesis of 3-dimensional (3D) networks. Attempts to obtain a 3D structure by using oxalate ions as bridging ligands have been recently reported in the literature [5–7]. These studies focused on the stoichiometric unit $\{[N(Bu)_4][M(II)M'(III)(ox)_3]\}$ where Bu = n-butyl, ox = oxalate, with the idea of assembling alternately two- and three-valent 3d-metal ions in extended networks. From stoichiometric arguments 2D and 3D networks are equally possible and, since no single crystals have been available, the question of dimensionality has not yet been solved.

*Author to whom correspondence should be addressed.

SSDI 0020-1693(93)03711-I

Without knowing the crystal structure of the compounds it is, in principle, difficult to analyse the mechanism leading to a magnetically ordered state. In this respect our report on the 3D structure of $\{[Fe(bipy)_3][Fe(II)_2(ox)_3]\}_n$, where bipy = 2,2'-bipyridine, has gained some significance in the field of magnetic molecular materials [10]. Along similar lines we now report on the results of the 2D structure of the title compound. The magnetic measurements reveal a ferromagnetic phase transition with a $T_c = 5.9$ K, nearly identical to the published data for the compound with an analogous stoichiometry but with the $[N(Bu)_4]^+$ cation [7]. Since the magnetic behaviour of the latter compound has been discussed in favour of a possible 3D structure, it should now be evident that the interpretation has to be done on the basis of a layered structure.

In addition, we have been interested in the optical properties of the mixed-metal compound. The single crystal absorption spectra reveal the expected results for tris-oxalato Cr(III) complexes with D_3 symmetry and the C_3 axis aligned parallel to the crystallographic c axis. At low temperature, a strong site selective luminescence from the Cr(III) ^2E states can be observed and the two-dimensional mixed-metal network structure is potentially interesting for the study of energy transfer mechanisms.

Experimental

Synthesis of $\{[P(Ph)_4][MnCr(ox)_3]\}_n$

All chemicals were of reagent grade and were used as commercially obtained. $K_3[Cr(ox)_3]\cdot 3H_2O$ was prepared according to literature methods [11]. Slow evaporation of an aqueous solution of equimolar quantities of $K_3[Cr(ox)_3]\cdot 3H_2O$, $MnCl_2\cdot 4H_2O$ and $P(Ph)_4Cl$ yielded the title compound in crystalline form. The dark blue crystals, with the morphology of capped hexagonal pyramids, show a distinct red–blue dichroism when examined under polarized light. *Anal.* Calc. for $C_{30}H_{20}O_{12}PCrMn$: C, 50.7, H, 2.8. Found: C, 51.0; H, 2.9%.

X-ray crystallographic analysis

A dark blue crystal of the title compound with approximate dimensions $0.17\times0.23\times0.33$ mm was selected for the X-ray measurements. Unit cell parameters were determined by least-squares refinement of 25 reflections in the interval $7.5<\theta<10.3°$ with $a = 18.774(3)$, $b = 18.786(3)$, $c = 21.947(8)$ Å, $\alpha = 64.73(2)$, $\beta = 64.73(2)$, $\gamma = 60.04(1)°$, $V = 5835(3)$ Å^3. 23 793 (including 294 standards) intensity data of this reduced cell were collected on an Enraf-Nonius CAD-4 diffractometer with graphite-monochromated Mo Kα radiation ($\lambda = 0.71073$ Å). Three standard reflections were monitored at an interval of every 3 h to check the crystal stability. The variation of standards was about 1.6%. To control the orientation, three standard reflections were collected every 400 reflections The intensities were corrected for Lorentz and polarization effects and a numerical absorption correction based on eight crystal faces was applied. The corrected data were transformed by a matrix (100, $\bar{1}10$, $\bar{1}\bar{1}3$), resulting in the possible rhombohedral space groups $R\bar{3}c$ and $R3c$, according to systematic extinction conditions for hexagonal settings. The new cell dimensions were $a = b = 18.783(3)$, $c = 57.283(24)$ Å. 1107 reflections with negative intensities were rejected from the data set, 22 392 data were merged, $R_{int} = 0.0697$, giving 5535 unique reflections. Further crystallographic details are given in Table 1. The structure could be solved in the space group $R3c$ by a Patterson synthesis using the program SHELXS-86 [12].

For good reasons the Patterson synthesis was started in the centrosymmetric space group $R\bar{3}c$. The solution however was chemically not meaningful, the reliability factor R_E was 64.7% based on 2513 E values (normalized structure factors) for 29 proposed atomic positions. R_E for the non-centrosymmetric solution ($R3c$) was 40.7%

TABLE 1. Crystal and refinement data for $\{[P(Ph)_4][MnCr(ox)_3]\}_n$

Chemical formula	$C_{30}H_{20}O_{12}PCrMn$
M_r	710.40
Crystal system	rhombohedric
Space group	$R3c$
$a = b$ (Å)	18 783(3)
c (Å)	57 283(24)
$\alpha = \beta$ (°)	90
γ (°)	120
V (Å^3)	17502(13)
Z	24
Crystal dimensions (mm)	0.17 × 0 23 × 0 33
Temperature (K)	295
$F(000)$ (electrons)	8640
ρ_{obs} (g cm^{-3})	1 60
ρ_{calc} (g cm^{-3})	1 618
λ(Mo Kα) (Å)	0.71073
μ (cm^{-1})	8.96
Scan type	$\omega/2\theta$
Variable scan speed (°/min)	1.50–5 49
Max measuring time (s)	50
Scan width (°)	0.80 + 0.35tgθ
2θ min–max. (°)	2 0–52.0
Reflections measured/unique	23499/5535
Reflections with $F_o > 3\sigma(F_o)$	3654
Absorption correction	numerical
Max./min transmission coefficients	0 8474/0.7768
Extinction correction	none
R/R_w	0.108/0.082
Goodness of fit	3.083
Largest shift/e.d s., final cycle	0 074
Max and min residual density (e/Å^3)	1.047/ − 1 370

for 2513 E values and for 38 atomic positions. The two-dimensional network of the structure was clearly shown. 28 missing carbon atomic positions of the phenyl groups were subsequently found in difference electron density maps. The positions of the Mn and Cr atoms were assigned by metal–oxygen distances criteria: Mn–O distances of 2.158 Å were found in a recently refined three-dimensional cubic network of $\{[Ni(bipy)_3][Mn(II)_2(ox)_3]\}_n$ [13], and Cr–O distances of about 1.97 Å were found in the literature [14]. All Mn–O distances of the title structure found in the Patterson interpretation map of SHELXS-86 were between 2.10 and 2.16 Å, and the Cr–O lengths were between 1.94 and 2.06 Å. After completing the structure by difference Fourier calculations, the phenyl rings were refined as rigid groups with C–C distances of 1.395 Å and C–C–C angles of 120°. As the hydrogen atomic positions could not be found by difference Fourier calculations, they were calculated geometrically and were refined also as rigid groups with C–H bond lengths of 0.96 Å with free isotropic displacement parameters.

The absolute polarity of the structure was then determined by using Flack's x-parameter refinement [15] with the γ-test version of the program SHELXL-93 [16]. After inverting the atomic coordinates, the x-parameter refined finally to 0.005(133). According to the paper of Glazer and Stadnicka [17], the absolute morphology of the title structure can be determined in combination by using Flack's x-parameter refinement and indexing the crystal faces (done with the MICROR/MICROS routines of Enraf-Nonius MOLEN software [18]): the crystal was oriented with its large face (006) on top and the small face (006) in contact with the glass fibre. The orientation of the phenyl rings in the structure ([110] projection, see Fig. 4) is in accordance with these observations.

In the final full-matrix refinement with SHELXTL-PLUS-88 [19] 3597 significant observed reflections were used and 395 parameters were varied. Because of the poor parameter-to-data ratio, only the Cr, Mn, P and O atoms were refined with anisotropic displacement parameters. Of the 36 phenyl-carbon atoms, 22 were refined anisotropically. Altogether, of 96 atoms, 23 carbons and 40 hydrogen atoms were refined isotropically. The refinement was stopped at a maximum shift/error ratio of 0.074 with R/R_w values of 10.79/8.17%. The weighting scheme used was $w=1/\sigma^2(F_o)$. Final positional and isotropic (U_{iso}) or equivalent isotropic (U_{eq}) displacement parameters are given in Table 2.

Magnetic measurements

The magnetic susceptibility data of a powdered sample were collected between 260 and 4.2 K with a vibrating-sample magnetometer (Foner magnetometer, Princeton Applied Research), which was operated at 0.2 T. The

TABLE 2. Atomic coordinates and equivalent isotropic displacement parameters (Å^2) for the non-hydrogen atoms of $\{[P(Ph)_4][MnCr(ox)_3]\}_n$

Atom	x/a	y/b	z/c	U_{eq}[a]/U_{iso}[b]
Mn1	1 0000	1.0000	0.9998	0 0135(9)
Cr1	0 8156(2)	0 6671(2)	0 99832(9)	0.033(1)
Mn2	0 4812(2)	0.4820(2)	0 9973(1)	0.063(1)
Cr2	0 3333	0 6667	0.9962(2)	0.117(4)
O11	0 9028(6)	0 9031(7)	1.0180(2)	0 033(5)
O21	0 9773(6)	0.8980(6)	0.9779(2)	0.026(5)
O31	0 8990(5)	0 7616(6)	0.9787(2)	0 026(5)
O41	0 8266(7)	0.7668(7)	1.0163(2)	0 031(5)
C11	0 8829(10)	0 8345(10)	1.0095(3)	0 030(4)*
C21	0.9202(11)	0.8269(10)	0.9871(3)	0 037(4)*
O12	0.9016(7)	0.6669(6)	1.0169(3)	0.061(6)
O22	0.8309(8)	0.5847(6)	0.9789(3)	0 044(6)
O32	0 9066(9)	0.5272(8)	0 9780(3)	0 058(8)
O42	0 9821(9)	0.6020(8)	1 0177(3)	0.057(7)
C12	0 9309(10)	0 6145(10)	1.0081(3)	0 032(4)*
C22	0 8868(11)	0 5723(11)	0.9854(4)	0 045(5)*
O13	0 7179(7)	0 6509(7)	0 9785(3)	0 046(6)
O23	0 7253(8)	0 5792(7)	1.0179(3)	0.050(6)
O33	0 5853(9)	0.5050(8)	1.0179(3)	0 070(8)
O43	0 5828(7)	0.5715(8)	0.9779(2)	0 052(7)
C13	0.6471(10)	0 5950(10)	0.9848(4)	0 038(4)*
C23	0.6532(11)	0.5557(11)	1 0087(4)	0.045(5)*
O14	0 3547(12)	0.7657(11)	1.0153(3)	0 099(11)
O24	0 2409(11)	0.6644(11)	0.9770(4)	0 090(10)
O34	0 0995(10)	0.6056(10)	0 9766(3)	0.083(10)
O44	0.1005(10)	0.5287(10)	1 0180(3)	0.079(9)
C14	0 1716(12)	0.5735(11)	1.0094(4)	0 040(4)*
C24	0 1693(17)	0.6206(16)	0.9859(5)	0.078(7)*
P1	1 0000	1.0000	1.0998(2)	0.037(2)
C211	1.0610(8)	0 8958(8)	1.0990(2)	0.071(13)
C311	1 0720(8)	0.8329(8)	1.0900(2)	0 094(8)*
C411	1.0262(8)	0 7876(8)	1.0708(2)	0 070(6)*
C511	0 9695(8)	0 8052(8)	1.0605(2)	0 078(6)*
C611	0.9585(8)	0.8681(8)	1.0695(2)	0 052(9)
C111	1 0042(8)	0.9134(8)	1.0887(2)	0 044(9)
C212	0 9487(25)	0.9226(21)	1.1413(5)	0.053(14)*
C312	0 9422(25)	0.9223(21)	1.1656(5)	0.012(8)*
C412	0.9901(25)	0.9944(21)	1.1782(5)	0 025(9)*
C512	1 0444(25)	1 0667(21)	1.1666(5)	0 31(11)*
C612	1 0509(25)	1.0670(21)	1.1423(5)	0 067(17)*
C112	1 0031(25)	0.9950(21)	1.1297(5)	0 035(9)*
P2	0.6698(3)	0.8301(2)	0.9329(1)	0 037(2)
C221	0.6152(6)	0.7668(5)	0.9770(2)	0.065(5)*
C321	0.6183(6)	0.7690(5)	1.0014(2)	0.098(9)*
C421	0 6761(6)	0.8402(5)	1.0128(2)	0.100(14)
C521	0.7308(6)	0 9092(5)	0 9999(2)	0.052(9)
C621	0 7277(6)	0.9069(5)	0.9756(2)	0 076(10)
C121	0 6699(6)	0.8357(5)	0.9642(2)	0 035(6)
C222	0 6344(9)	0 9561(9)	0.9344(2)	0.099(20)
C322	0.6297(9)	1.0227(9)	0.9255(2)	0.093(17)
C422	0 6594(9)	1.0522(9)	0.9031(2)	0.084(7)*
C522	0.6938(9)	1 0150(9)	0.8897(2)	0.088(14)
C622	0.6984(9)	0.9484(9)	0.8986(2)	0 086(12)
C122	0 6688(9)	0.9189(9)	0 9210(2)	0.048(9)
C223	0 8316(8)	0.8625(10)	0.9359(2)	0.088(15)
C323	0 9023(8)	0.8693(10)	0.9258(2)	0 194(35)
C423	0 9001(8)	0 8432(10)	0.9028(2)	0.082(14)
C523	0 8273(8)	0 8102(10)	0.8900(2)	0 079(7)*

(*continued*)

TABLE 2 (*continued*)

Atom	*x/a*	*y/b*	*z/c*	U_{eq}^{a}/U_{iso}^{b}
C623	0.7566(8)	0 8034(10)	0 9002(2)	0 056(10)
C123	0 7587(8)	0 8296(10)	0.9231(2)	0.032(7)
C224	0 5779(8)	0.6629(8)	0.9266(3)	0 079(7)*
C324	0.5169(8)	0.5925(8)	0.9156(3)	0 124(17)
C424	0.4586(8)	0 5973(8)	0 9016(3)	0 110(15)
C524	0 4613(8)	0.6724(8)	0 8987(3)	0.303(35)
C624	0.5224(8)	0.7427(8)	0 9097(3)	0 218(33)
C124	0.5807(8)	0.7379(8)	0 9237(3)	0 036(4)*

$^{a}U_{eq} = \frac{1}{3} \Sigma_i \Sigma_j U_{ij} a_i^* a_j^* \mathbf{a}_i \mathbf{a}_j$. ^{b}Starred atoms were refined isotropically.

instrument was calibrated with $Hg[Co(NCS)_4]$. The diamagnetic correction was estimated from Pascal's constants to be -340×10^{-6} cm^3 mol^{-1}. The magnetization of the compound was measured as a function of the magnetic field at 4.2 K; the range of applied fields was 0.01–1.8 T. The spontaneous magnetization was determined by slowly cooling the sample down to 4.2 K in zero field. However the field control of the magnet is not optimal in the low to zero field range, therefore a small residual field of some Gauss may still operate on the samples.

Optical measurements

Polarized single crystal absorption spectra were recorded on a Cary 5e spectrometer, with the samples mounted in a closed cycle cryostat (Air Products) for temperatures down to 12 K, and using a pair of matched Glan-Taylor polarizers. Luminescence spectra were recorded on a set-up previously described [20]. For excitation, the 568 nm line (5 mW) from a Kr^+ laser (Coherent Innova 300 K) was used, and samples were cooled to 5 K in a cold helium gas flow.

Results and discussion

Crystal structure

The declared interest for the structural details of a polymeric $[MM'(ox)_3]_n$ lattice stems from the potential for the '$[M(ox)_3]$ building block complex' to build two- or three-dimensional networks. By representing the trischelated $[M(ox)_3]$ complexes by octahedra and assigning the two possible chiralities as Λ and Δ, both structure types may easily be visualized. By using an alternating assembly of the two types of chiral octahedra, a 2D honey-combed layered structure is always generated, while using just Λ or Δ octahedra results in the enantiomorphic 3D lattice [10].

For the title compound the structure analysis reveals an anionic, two-dimensional network with the stoichiometry $[Mn(II)Cr(III)(ox)_3]_n^{n-}$ and a slightly distorted hexagonal pattern. The $[P(Ph)_4]^+$ cations are located between these layers, which are thereby separated by about 9.5 Å. The space group requires six pairs of anionic and cationic layers per unit cell. The sequence of these 'bilayers' is given by the space group symmetry operators. Figure 1 shows a thermal ellipsoid plot of the manganese and chromium coordination from the zero layer of the unit cell. The labelled atoms have been individually refined. Mn1 and Cr2 are lying on special sites with a three-fold axis (Wyckoff letter a), whereas Mn2 and Cr1 are located in general positions. Selected bond lengths and interbond angles are given in Table 3. The Mn(II)–O bond distances with a mean value of 2.13(2) Å compare well with the mean value of 2.158(2) Å from the analogous bonds in the 3D network $\{[Ni(bipy)_3][Mn(II)_2(ox)_3]\}_n$ [13]. The Cr(III)–O bond distances, which are expected to be shorter, exhibit a mean value of 2.02(2) Å, comparable with the cited value of 1.972(5) Å in $[Cr(ox)_3]^{3-}$ [14]. These differences between the Mn–O and Cr–O bond lengths cause a slight distortion of the hexagonal pattern Figure 2 exhibits an overall view of the zero layer and the slightly elongated ellipsoids of the connected net are perceivable. The alternating chirality of the $[M(ox)_3]$ units can also be clearly seen.

The $[P(Ph)_4]^+$ cations are all arranged with one phosphorus–phenyl bond parallel to the crystallographic *c* axis. These phenyl groups, pointing vertically to the anionic layers, just fit into the ellipsoidic vacancies. There is one phosphorus atom (P1) lying on a special site with a three-fold axis and one phosphorus atom (P2) in a general position. In Fig. 3 a stereo plot of a trigonal environment including the cations is shown.

In Fig. 4, a [110] projection of the unit cell, presents the arrangement of the six anionic and cationic layers and illustrates their interconnectivity.

Magnetic measurements

The magnetic behaviour of the polycrystalline sample is shown in Fig. 5 in the form of $1/\chi_M$ versus T and μ_{eff} versus T plots. χ_M is the magnetic susceptibility per MnCr unit and μ_{eff} is the effective magnetic moment calculated by the equation $\mu_{eff} = 2.828(\chi_M T)^{1/2}$. The plot of $1/\chi_M$ versus T is linear in the range 260–20 K. The Weiss constant determined from this temperature range, based on the equation $1/\chi_M = C(T-\theta)$ is +10.5 K, which suggests the presence of a ferromagnetic interaction. The effective magnetic moment starts with a value of 7.2 μ_B at 260 K, increases gradually with cooling to 20 K and then rises sharply below 20 K to a value of over 45 μ_B at 4 2 K, which indicates the onset of ferromagnetism. The high value of μ_{eff} at 4.2 K must be compared with the max. spin-only value of $\mu_{eff} = 8.94$ μ_B for the total spin ($S_T = 4$) of an Mn(II)–Cr(III) pair.

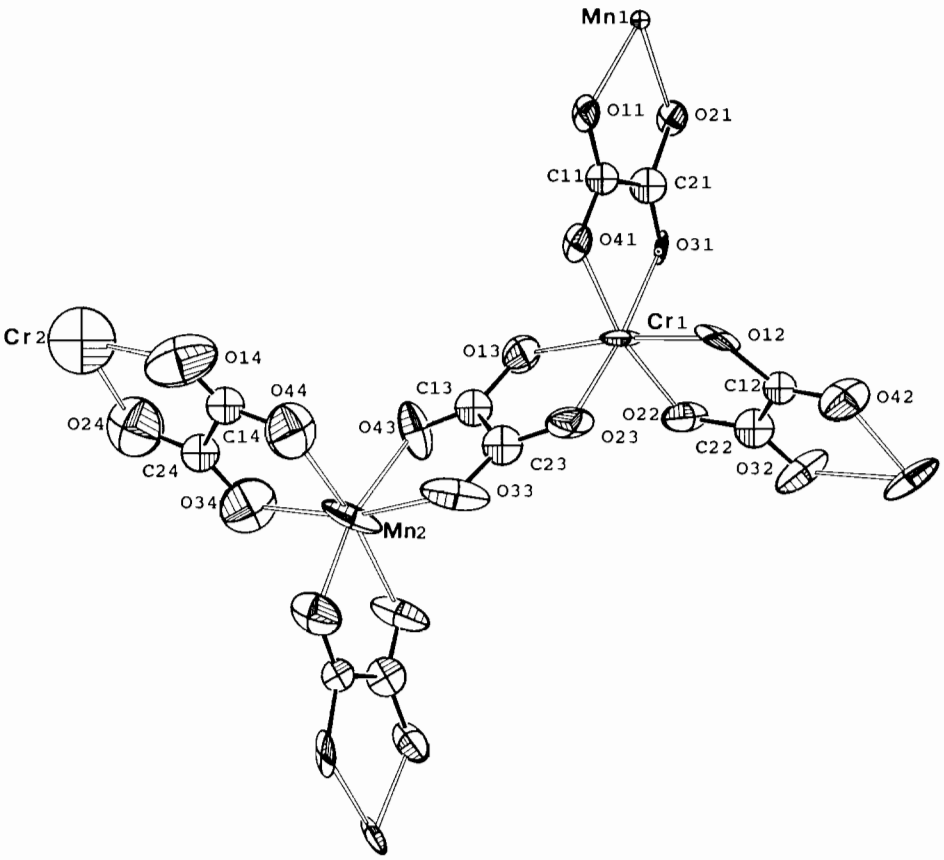

Fig. 1 ORTEP drawing (50% probability) of the Mn and Cr coordination in the two-dimensional network

The occurrence of a ferromagnetic phase transition is confirmed by the behaviour of the spontaneous magnetization (M) versus T curve shown in Fig. 6. When the sample is slowly cooled in a residual field of some Gauss (see 'Experimental'), a spontaneous magnetization appears with $T_c = 5.9$ K. The same phase transition was observed when the remnant magnetization of the sample vanished at T_c as the sample was warmed. We also measured, at 4.2 K, the variation of M as a function of the field (H) up to 1.8 Tesla (Fig. 7). The saturation magnetization (M_S) reaches a value of about 7.5 μ_B per MnCr unit at 1.8 T. This value is compatible with $S_T = 4$ and $g = 2$ for the equation $M_S = g\beta NS$ where S is the spin quantum number for a unit formula. Here we have again to stress the analogy with the published magnetic data on the same system but with $[N(Bu)_4]^+$ cations [7]. For this reason, also a structural similarity between these compounds can be deduced. Hence, the low T_c values exhibited by this kind of mixed-metal system have to be taken as a consequence of the 2D structure arrangement.

Whereas some models have been established in order to interpret the magnetic data for alternating bimetallic chains, this is not yet the case for bimetallic two-dimensional structures. In such cases, a cooperative magnetic ordering of the spins below T_c may have its origin from an anisotropy which is put into force at low temperature, as well as from interlayer interactions. Both effects must be very weak, since Mn(II) and Cr(III) usually exhibit no pronounced anisotropy, and the interlayer gap is rather wide and the structure reveals no favourable interlayer exchange pathway. This means that only low T_c values may result. In addition the argument about the type of magnetic ordering does not seem to be straightforward, since the Mn(II)–Cr(III) interaction has been expected to be antiferromagnetic [22]. Now that structural details of this kind of layered compound are known, further efforts may be made towards a clearer theoretical study of these properties.

Optical measurements

The polarized single crystal absorption spectra of the title compound correspond to the ones for $[Cr(ox)_3]^{3-}$ doped into $NaMg[Al(ox)_3]\cdot 8H_2O$ [23]. At 12 K the broad bands corresponding to the $^4A_2 \rightarrow {}^4T_2$ and the $^4A_2 \rightarrow {}^4T_1$ transitions are centred at 17 580 cm^{-1} ($\epsilon_\pi = 105$ M^{-1} cm^{-1}, $\epsilon_\sigma = 75$ M^{-1} cm^{-1}) and 23 550 cm^{-1} ($\epsilon_\pi = 27$ M^{-1} cm^{-1}, $\epsilon_\sigma = 245$ M^{-1} cm^{-1}), respectively. π and σ refer to the electric vector of linearly polarized light parallel or perpendicular to the trigonal

TABLE 3 Relevant bond length (Å) and angles (°) for $\{[P(Ph)_4][MnCr(ox)_3]\}_n$

Mn1–O11 3×	2.100(10)	Mn1–O21 3×	2 147(12)
Cr1–O31	2 023(10)	Cr1–O41	2 054(14)
Cr1–O12	1 935(15)	Cr1–O22	2.040(15)
Cr1–O13	2 047(15)	Cr1–O23	2 014(12)
Mn2–O33	2 134(18)	Mn2–O43	2 121(12)
Mn2–O32$^{(i)}$	2 158(18)	Mn2–O42$^{(i)}$	2.118(14)
Mn2–O34$^{(i)}$	2 115(21)	Mn2–O44$^{(i)}$	2 146(21)
Cr2–O14 3×	2 016(21)	Cr2–O24 3×	2 039(23)
C11–O11	1 247(22)	C11–O41	1 240(17)
C11–C21	1.503(28)	C21–O21	1 335(17)
C21–O31	1.185(21)		
C12–O12	1.437(27)	C12–O42	1 230(28)
C12–C22	1.533(27)	C22–O22	1 241(29)
C22–O32	1.160(31)		
C13–O13	1.269(18)	C13–O43	1 131(23)
C13–C23	1 584(31)	C23–O23	1 307(25)
C23–O33	1 264(22)		
C14–O14	1 114(27)	C14–O44	1 269(24)
C14–C24	1 627(38)	C24–O24	1 280(31)
C24–O34	1 308(37)		
P1–C111	1 783(17) 3×	P1–C112	1 719(29)
P2–C121	1 794(14)	P2–C122	1 810(19)
P2–C123	1.767(18)	P2–C124	1 784(12)
O11–Mn1–O21	79 5(4)	O11–Mn1–O11$^{(i)}$	97 5(4)
O21–Mn1–O11$^{(i)}$	94 2(5)	O11–Mn1–O11$^{(ii)}$	97.5(5)
O21–Mn1–O11$^{(ii)}$	168 2(4)	O11$^{(i)}$–Mn1–O11$^{(ii)}$	97 5(4)
O11–Mn1–O21$^{(i)}$	168 2(5)	O21–Mn1–O21$^{(i)}$	89 3(4)
O11$^{(i)}$–Mn1–O21$^{(i)}$	79 5(5)	O11$^{(ii)}$–Mn1–O21$^{(i)}$	94 2(5)
O11–Mn1–O21$^{(ii)}$	94 2(5)	O21–Mn1–O21$^{(ii)}$	89 3(4)
O11$^{(i)}$–Mn1–O21$^{(ii)}$	168 2(4)	O11$^{(ii)}$–Mn1–O21$^{(ii)}$	79 5(4)
O21$^{(i)}$–Mn1–O21$^{(ii)}$	89 3(5)		
O31–Cr1–O41	78 2(5)	O31–Cr1–O12	91 5(5)
O41–Cr1–O12	91 4(6)	O31–Cr1–O22	91 2(5)
O41–Cr1–O22	167 5(4)	O12–Cr1–O22	82 1(6)
O31–Cr1–O13	93.7(5)	O41–Cr1–O13	95 0(6)
O12–Cr1–O13	172.5(5)	O22–Cr1–O13	92 3(6)
O31–Cr1–O23	173 8(6)	O41–Cr1–O23	97 4(5)
O12–Cr1–O23	93.1(6)	O22–Cr1–O23	93 5(5)
O13–Cr1–O23	82.1(6)		
O33–Mn2–O43	76.1(5)	O33–Mn2–O32$^{(iii)}$	96 6(6)
O43–Mn2–O32$^{(iii)}$	94.3(6)	O33–Mn2–O42$^{(iii)}$	93.7(6)
O43–Mn2–O42$^{(iii)}$	166 3(7)	O32$^{(iii)}$–Mn2–O42$^{(iii)}$	77 6(6)
O33–Mn2–O34$^{(v)}$	164 6(6)	O43–Mn2–O34$^{(v)}$	93 3(6)
O32$^{(iii)}$–Mn2–O34$^{(v)}$	95.3(7)	O42$^{(iii)}$–Mn2–O34$^{(v)}$	98.4(6)
O33–Mn2–O44$^{(v)}$	88.0(7)	O43–Mn2–O44$^{(v)}$	93 7(6)
O32$^{(iii)}$–Mn2–O44$^{(v)}$	171 5(5)	O42$^{(iii)}$–Mn2–O44$^{(v)}$	95 1(7)
O34$^{(v)}$–Mn2–O44$^{(v)}$	81.5(8)		
O14–Cr2–O24	95 0(9)	O14–Cr2–O14$^{(v)}$	93 4(7)
O24–Cr2–O14$^{(v)}$	79 0(8)	O14–Cr2–O14$^{(iv)}$	93 4(8)
O24–Cr2–O14$^{(iv)}$	169 0(8)	O14$^{(v)}$–Cr2–O14$^{(iv)}$	93 4(9)
O14–Cr2–O24$^{(v)}$	169.0(8)	O24–Cr2–O24$^{(v)}$	93 6(8)
O14$^{(v)}$–Cr2–O24$^{(v)}$	95 0(8)	O14$^{(iv)}$–Cr2–O24$^{(v)}$	79 0(8)
O14–Cr2–O24$^{(iv)}$	79.0(7)	O24–Cr2–O24$^{(iv)}$	93.6(9)
O14$^{(v)}$–Cr2–O24$^{(iv)}$	169.0(8)	O14$^{(iv)}$–Cr2–O24$^{(iv)}$	95.0(7)
O24$^{(v)}$–Cr2–O24$^{(iv)}$	93 6(9)		

Symmetry operators: (i) = $2-y$, $1+x-y$, z, (ii) = $1-x+y$, $2-x$, z, (iii) = $1-y$, $x-y$, z; (iv) = $-x+y$, $1-x$, z, (v) = $1-y$, $1+x-y$, z.

molecular axis, which corresponds to the crystallographic c axis. The α-spectrum, measured with light propagating along this axis, matches the polarization relationships of the σ-spectrum. The distinct polarization behaviour of the $^4T_1$ absorption band corresponds with the selection rules for electric dipole transitions in D_3 symmetry and is also the origin of the observed dichroism. This reflects the parallel alignment of the trigonal molecular axes from the individual $[Cr(ox)_3]$ units which is in accordance with the 2D structure model. The spin-forbidden tran-

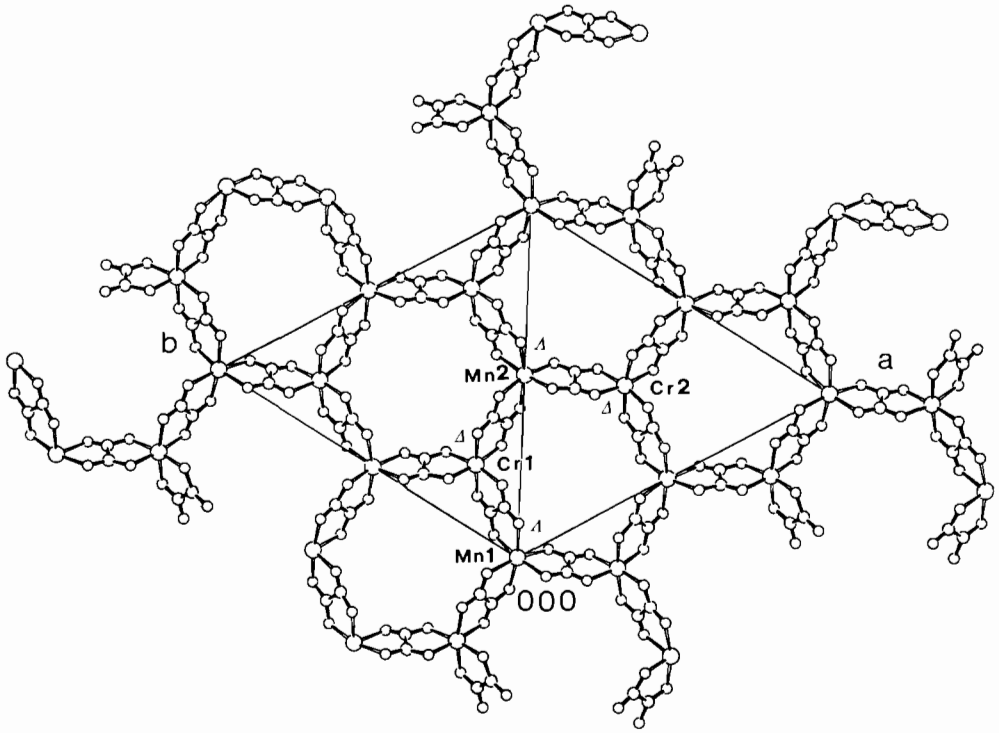

Fig 2 Sector from the $[MnCr(ox)_3]_n$ zero layer [21]

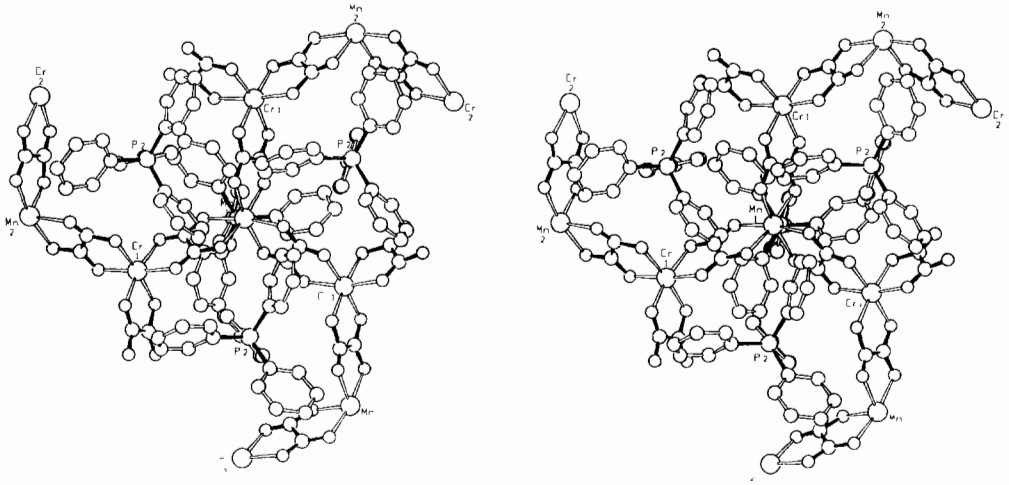

Fig 3 Stereo plot of a trigonal environment including the cations

sitions $^4A_2 \rightarrow {}^2E$, $^4A_2 \rightarrow {}^2T_1$ and $^4A_2 \rightarrow {}^2T_2$ are observed as sharp features at approximately the same energies as in the host matrix cited above.

$\{[P(Ph)_4][MnCr(ox)_3]\}_n$ luminesces strongly at low temperatures. Figure 8 shows the region of the electronic origins of the $^2E \rightarrow {}^4A_2$ transitions. As the temperature is raised from 5 K, a hot band develops on the high energy side. At the same time the total intensity drops very quickly. From the hot band we estimate a splitting of the ^2E state of ≈ 20 cm^{-1}. The interaction between neighbouring paramagnetic metal centres gives rise to the observed magnetic behaviour and also to energy transfer processes. Because of the small horizontal shift of the ^2E and $^4A_2$ states relative to each other and the resulting large spectral overlap between absorption and luminescence, we would expect this energy transfer to be very efficient down to low temperatures [24]. The rapid quenching of the luminescence at comparatively low temperatures is a strong indication that this is indeed what is happening. Further complications arise from the fact that the Cr(III) ions occupy two crystallographically non-equivalent sites. Even at 5 K the

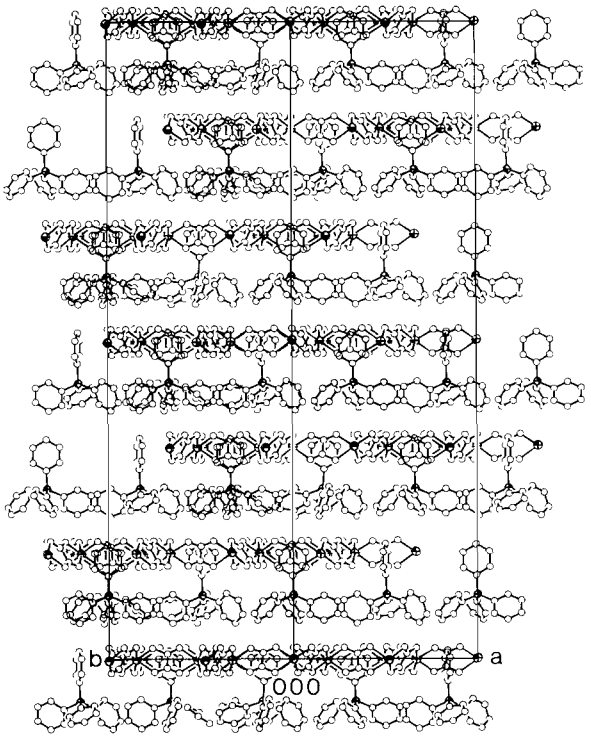

Fig 4 [110] projection of $\{[P(Ph)_4][MnCr(ox)_3]\}_n$.

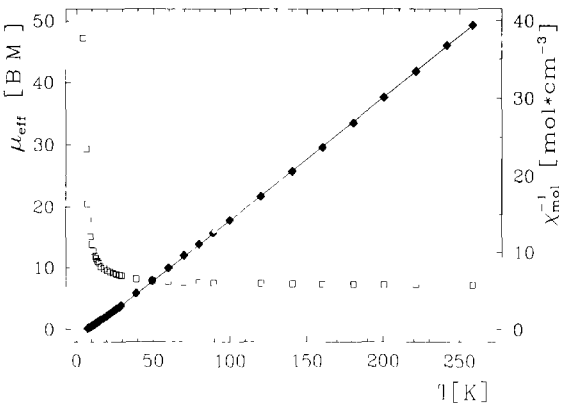

Fig. 5 Temperature dependences of inverse magnetic susceptibility $1/\chi_M$ (◆) and effective magnetic moment μ_{eff} (□) per MnCr of $\{[P(Ph)_4][MnCr(ox)_3]\}_n$

energy transfer must still be efficient, as the observed luminescence seems mostly due to just one site.

Further work is needed, for instance on dilute samples, in order to understand the energy transfer phenomena in these network structures. Of particular interest, both with respect to the energy transfer as well as to the magnetic properties, would be the role of the divalent bridging metal. Site selective excitation and luminescence line narrowing techniques, as well as time resolved methods, would help to differentiate between the non-equivalent lattice sites spectroscopically and yield information on the dynamics of the system [25].

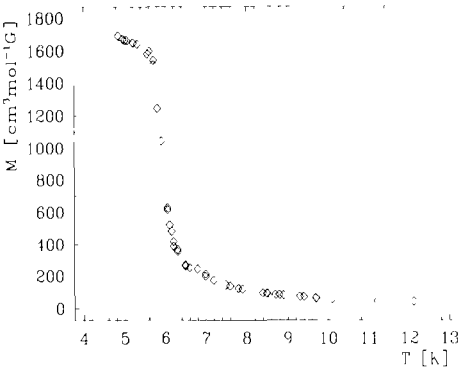

Fig 6. Temperature dependence of the spontaneous magnetization M for $\{[P(Ph)_4][MnCr(ox)_3]\}_n$

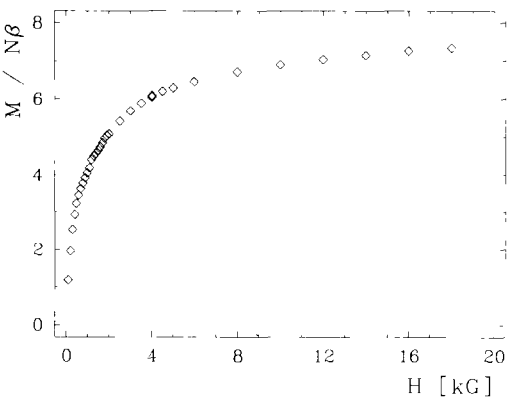

Fig. 7 Field dependence of the magnetization M for $\{[P(Ph)_4][MnCr(ox)_3]\}_n$ at 4 2 K

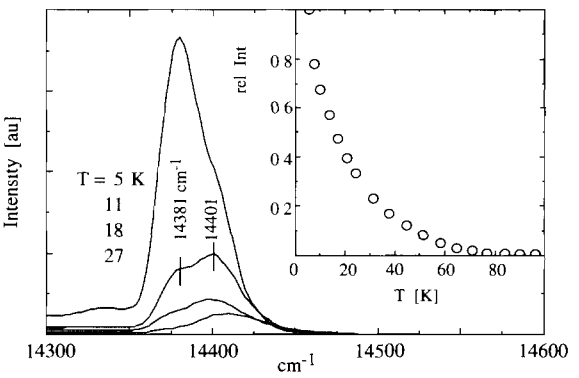

Fig. 8. Luminescence in the region of electronic origins of the $^2E \rightarrow {}^4A_2$ transitions of $\{[P(Ph)_4][MnCr(ox)_3]\}_n$ at 5, 11, 18 and 27 K Insert: temperature dependence of the luminescence intensity

Conclusions

With this and a previous report [10], a two- and three-dimensional polymeric structure of 3d-metal ions bridged by chelating oxalate ligands and the stoichiometric unit $[MM'(ox)_3]$ have been presented. The counterions, $[P(Ph)_4]^+$ in the former and $[M(bipy)_3]^{2+}$ in the latter case, may play a dominating role in the

crystal packing, thus directing the structure towards a 2D or 3D network. Further studies to clarify the structural versatility of these systems are in progress in our laboratory. In addition, there is an interest in studying the magnetic behaviour of these polymeric networks with a view towards applications for molecular based magnets as well as model systems which facilitate a better understanding of two- and three-dimensional lattices. Also in this respect, more data on analogous, chemically modified compounds are needed in order to tackle successfully the interpretation of the magnetic interactions which are occurring.

Supplementary material

Supplementary material including tables of observed and calculated structure factors, of anisotropic thermal parameters, a stereo plot of the unit cell and 6 SCHAKAL plots of the individual layers of the anionic nets may be obtained on request from author H.W.S.; additional material (bond distances and angles) can be ordered from the Fachinformationszentrum Karlsruhe, D-76344 Eggenstein-Leopoldshafen, Germany. Please quote reference No. CSD-57460, the names of authors and the title of the paper.

Acknowledgement

Gratitude is expressed to the Swiss National Science Foundation for financial support under Project No. 20-34063.92.

References

1 M Verdaguer, A. Gleizes, J.P. Renard and J. Seiden, *Phys Rev B, 29* (1984) 5144
2 O Kahn, Y Pei, M Verdaguer, J.P Renard and J. Sletten, *J Am Chem Soc, 110* (1988) 782
3 K. Nakatani, P. Bergerat, E Codjovi, C. Mathonière, Y. Pei and O Kahn, *Inorg Chem, 30* (1991) 3977
4 Y Pei, O. Kahn, K. Nakatani, E Codjovi, C. Mathonière and J. Sletten, *J Am. Chem Soc, 113* (1991) 6558
5 Z.J Zhong, N. Matsumoto, H Okawa and S. Kida, *Chem Lett*, (1990) 87
6 H Tamaki, M. Mitsumi, K. Nakamura, N Matsumoto, S. Kida, H. Okawa and S. Iijima, *Chem Lett*, (1992) 1975
7 H Tamaki, Z J. Zhong, N. Matsumoto, S Kida, M. Koikawa, N Achiwa, Y Hashimoto and H. Okawa, *J Am Chem. Soc., 114* (1992) 6974
8 V. Gadet, T. Mallah, I Castro, M. Verdaguer and P. Veillet, *J Am Chem Soc, 114* (1992) 9213
9 D Gatteschi, O. Kahn, J S. Miller and F. Palacio (eds), *Magnetic Molecular Materials,* NATO ASI Series, Vol. 198, Kluwer, Dordrecht, Netherlands, 1991.
10 S Decurtins, H W Schmalle, P. Schneuwly and H R Oswald, *Inorg Chem, 32* (1993) 1888
11 J C Bailar and E M Jones, in H S Booth (ed.), *Inorganic Syntheses,* Vol. 1, McGraw-Hill, New York, 1939, p. 37.
12 G.M Sheldrick, *Acta Crystallogr, Sect A, 46* (1990) 467
13 P. Schneuwly, *Ph D Thesis* (in progress), University of Zurich, Switzerland.
14 L. Golic and N Bulc, *Acta Crystallogr, Sect C, 44* (1988) 2065
15 G Bernardinelli and H D. Flack, *Acta Crystallogr., Sect A, 41* (1985) 500
16 G M Sheldrick, *J Appl Crystallogr*, (1993) in preparation.
17 A M Glazer and K. Stadnicka, *Acta Crystallogr, Sect A, 45* (1989) 234
18 Enraf-Nonius, *MOLEN,* an interactive structure solution procedure, Delft, Netherlands, 1990
19 G.M Sheldrick, *SHELXTL-PLUS-88,* structure determination software programs. Nicolet Instrument Corp., Madison, WI, USA, 1988.
20 G. Frei, A. Zillian, A Raselli, H U Gudel and H.B Burgi, *Inorg Chem, 31* (1992) 4766
21 E Keller, *SCHAKAL86,* a Fortran program for the graphic representation of molecular and crystallographic models, *Chem Unserer Zeit, 20* (1986) 178
22 Y Pei, Y Journaux and O Kahn, *Inorg Chem, 28* (1989) 100.
23 T. Schonherr, J. Spanier and H.H Schmidtke, *J. Phys Chem., 93* (1989) 5969.
24 D.L Dexter, *J Chem Phys, 21* (1953) 836.
25 H. Riesen and E. Krausz, *Comments Inorg. Chem, 14* (1993) 323.